



Metal complexes with superoxide dismutase-like activity as candidates for anti-prion drug

Tomoko Fukuuchi,^{a,b,*} Katsumi Doh-ura,^c Shin'ichi Yoshihara^b and Shigeru Ohta^a

^aGraduate School of Biomedical Sciences, Hiroshima University, 1-2-3 Kasumi, Minami-ku, Hiroshima 734-8553, Japan

^bFaculty of Pharmaceutical Sciences, Hiroshima International University, 5-1-1 Koshingai, Hiro, Kure, Hiroshima 737-0112, Japan

^cGraduate School of Medicine, Tohoku University, 2-1 Seiryō-cho, Aoba-ku, Sendai 980-8575, Japan

Received 28 July 2006; revised 29 August 2006; accepted 30 August 2006

Available online 20 September 2006

Abstract—Various compounds were evaluated for ability to inhibit the formation of the abnormal protease-resistant form of prion protein (PrP-res) in two cell lines infected with different prion strains. Examination of the structure–activity relationships indicated that compounds with copper-selective chelating ability and whose copper complexes have high SOD-like activity are candidates for anti-prion drug.

© 2006 Elsevier Ltd. All rights reserved.

Transmissible spongiform encephalopathies (TSEs) or prion diseases are a group of fatal neurodegenerative disorders, and their development is associated with accumulation of aggregated proteins, oxidative damage to the brain, and neuronal cell loss. Prion diseases are characterized by the generation of a protein molecule termed PrP^{Sc} (scrapie isoform of the prion protein), which is a conformational variant of the normal host protein, PrP^C (cellular isoform of the prion protein).^{1,2} It is believed that the conversion of PrP^C into PrP^{Sc} is the key event in the pathogenesis of TSEs.

The octapeptide repeat region of the PrP^C binds several copper ions with concentration of the micromolar range^{3,4} and their dissociation constant for the ion is reported to be femtomolar range.⁵ The biological significance of this interaction is not clear, but it is reported that PrP^C has a copper-dependent superoxide dismutase (SOD) activity⁶ and PrP^C may be involved in copper uptake into cells.^{7,8} Recently, there has been increasing interest in the role of metal ions, in particular copper, in prion diseases.^{9,10}

In the early 1970s, it was reported that the copper chelator cuprizone induced prion diseases-like histopa-

thological changes in mice.^{11,12} On the other hand, Sigurdsson et al. recently found that a copper chelator, D-penicillamine, delayed the onset of prion disease in infected mice, and suggested that chelator-based therapy might attenuate the disease.¹³ Copper has been implicated in the pathogenesis of prion disease, but numerous studies have only succeeded in demonstrating the complexity of the effects of copper on the development of prion diseases, and it remains unclear whether this ion promotes or inhibits disease progression.

In the present study, we evaluated the ability of a wide range of compounds¹⁴ to inhibit the formation of the abnormal protease-resistant form of prion protein (PrP-res), using two cell lines, ScN2a cells and F3, infected with different prion strains.^{15,16} We then analyzed the structure–activity relationships to investigate what kinds of structure or biochemical characteristics contribute to anti-prion activity.

Spectrophotometric complexation studies.^{17–19} The complexes were prepared as previously reported.^{20,21} Solutions of 10 mM Cu(ClO₄)₂ and 8-hydroxyquinoline were prepared in H₂O. Cu(II)-chelate formation of 8-hydroxyquinoline was demonstrated by Job's method.^{18,19} The spectrophotometric complexation studies showed that 8-hydroxyquinoline binds in 2:1 ratio with Cu(II) (Fig. 1A). 2,2'-Biquinoline, neocuproine, bathocuproine, 4,4'-dicarboxy-2,2'-biquinoline, porphyrins, cimetidine and D-penicillamine bind in 1:1 ratio with Cu(II) (2,2'-biquinoline, Fig. 1B; others, data not

Keywords: Prion; 2,2'-Biquinoline; Cimetidine; TPEN; Copper; Chelate; Metal complex; SOD activity.

* Corresponding author. Tel./fax: +81 823 73 8573; e-mail: t-fukuu@ps.hirokoku-u.ac.jp

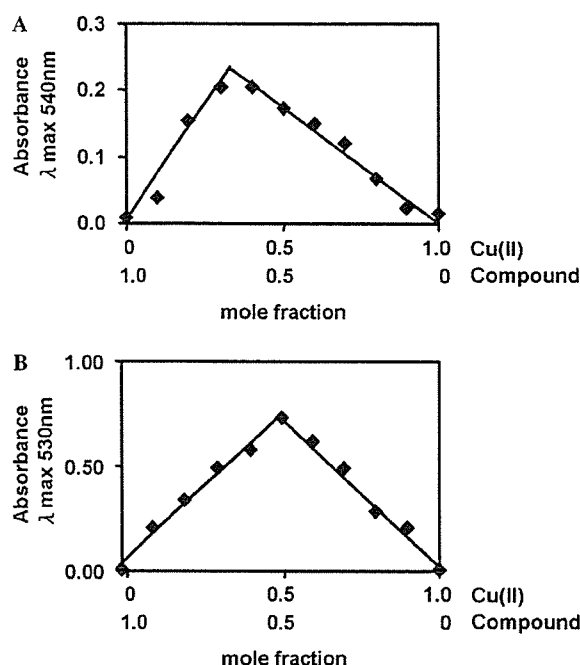


Figure 1. Continuous variation plots for 8-hydroxyquinoline and Cu(II) (A) and 2,2'-biquinoline and Cu(II) (B). (A) 2:1 binding ratio between 8-hydroxyquinoline and Cu(II), (B) 1:1 binding ratio between 2,2'-biquinoline and Cu(II). The plots were obtained by Job's method in aqueous solution.

shown). However, it has been reported that the oxidation state of copper may be altered in the D-penicillamine complex, and the complex prepared in this way contains both Cu(I) and Cu(II).²²

Inhibition of PrP-res formation in ScN2a cells and F3 cells by metal chelators.^{23–26} 1,10-Phenanthroline, 2,2',2''-terpyridine and 8-hydroxyquinoline did not inhibit PrP-res formation within a nontoxic dose range (Table 1), but were cytotoxic at 100 nM. Chelators of this class can chelate a wide variety of metals.

Neocuproine, bathocuproine, 2,2'-biquinoline and 4,4'-dicarboxy-2,2'-biquinoline are highly specific copper chelators. The chelators of this class, except 4,4'-dicarboxy-2,2'-biquinoline, effectively inhibited PrP-res formation in ScN2a cells and F3 cells in a dose-dependent manner (Fig. 2). The concentrations giving 50% inhibition (IC₅₀) of PrP-res formation in ScN2a cells relative to the DMSO-treated or untreated control ranged from 5 to 80 nM (Table 1). These compounds showed no apparent cytotoxicity at concentrations up to 1 μM. However, neocuproine was ineffective in F3 cells within a nontoxic dose range. Findings from these experiments suggest that compounds having copper-selective chelating ability are more effective inhibitors than non-selective metal-chelating compounds, but not an exclusive factor.

Inhibition of PrP-res formation in ScN2a cells and F3 cells by porphyrins.^{23–26} Porphyrins can form 1:1 stable chelates with various metal ions. The order of stability

for divalent metal ions is Cu > Fe > Zn > Mn, regardless of the type of substituents on the porphyrin ring. Porphyrins were effective inhibitors of PrP-res formation, with IC₅₀ values ranging from 5 to 320 nM in ScN2a cells and F3 cells (Table 2). And Mn(III)-porphyrins complexes showed higher anti-prion activity than the metal-free compounds (Table 2).

SOD-like activity and correlation with anti-prion activity. It is known that Mn(III)-porphyrin complexes show high SOD-like activity in vitro and in vivo.^{27,28} We thought that SOD-like activity might contribute to the anti-prion activity of such compounds, since the SOD activity of PrP^C is decreased by conversion to PrP^{Sc}. Therefore, we focused on chelators having SOD-like activity. Many low-molecular metal complexes, mainly copper, manganese and iron complexes, have been synthesized and their SOD-like activity examined in vitro and in vivo,^{29–33} and some of them showed activity in vivo.^{34–36} As shown in Table 3, SOD-like activity of these compounds was measured in vitro by our methods.³⁷ The SOD-like activity in cell lysates was significantly increased when these metal-free compounds were added to the cell cultures (data not shown). Therefore, the chelators that showed anti-prion activity formed metal complexes and had SOD-like activity.

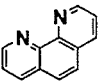
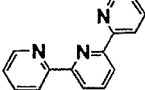
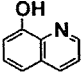
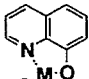
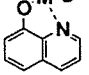
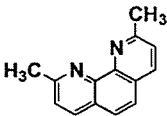
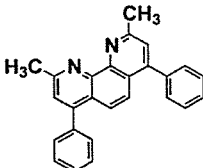
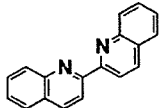
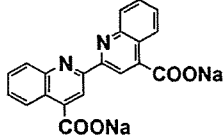
Among these compounds, we chose cimetidine^{34,38} and TPEN³⁹ for further examination, as well as Mn-TCPP (Mn-TBAP), which we had already examined. Cimetidine effectively inhibited PrP-res formation, with IC₅₀ values of 5 nM in ScN2a cells and 200 nM in F3 cells. TPEN inhibited PrP-res formation, with IC₅₀ values of 5 nM in ScN2a cells and 200 nM in F3 cells.

We found that the compounds, shown in Tables 1 and 2, with higher anti-prion activity in ScN2a cells had higher SOD-like activity (Table 3). Statistical analysis exhibited a significant linear correlation between these two activities ($r = 0.93$) (Fig. 3).

Despite numerous studies, it remains unclear whether copper ions promote¹³ or inhibit⁴⁰ prion disease. In Alzheimer's disease, another neurodegenerative disease, the copper- and zinc-selective chelator clioquinol was effective in decreasing β-amyloid deposits.⁴¹ However, Doh-ura et al. found that clioquinol and related compounds, quinoline hydrochloride, 8-hydroxyquinoline, and 8-acetoxyquinoline, were ineffective in scrapie-infected mouse neuroblastoma (ScNB) cells.²⁵ Thus, chelating drugs that are effective in inhibiting β-amyloid formation may not inhibit the conversion of PrP^C to PrP^{Sc}.

In this study, we evaluated the anti-prion activity of various compounds having metal-chelating ability in order to identify the requirements for anti-prion activity. We found that many, but not all, compounds having selective copper-chelating ability are effective inhibitors of PrP-res formation in ScN2a cells and F3 cells. Thus, copper-selective chelating ability per se may not be essential for anti-prion activity. This idea is supported by the observation that porphyrins chelating manganese

Table 1. Inhibition of PrP-res formation in ScN2a cells and F3 cells by metal chelators

Compound	Structure	Metal(M)	Inhibition PrP-res IC ₅₀ (nM)	
			ScN2a cells	F3 cells
1,10-Phenanthroline			N.E.	N.E.
2,2',2''-Terpyridine			N.E.	N.E.
8-Hydroxyquinoline			N.E.	N.E.
Bis(8-quinolinolato) Copper(II)		Cu ²⁺	N.E.	N.E.
Bis(8-quinolinolato) Zinc(II)		Zn ²⁺	N.E.	N.E.
Neocuproine			80	N.E.
Bathocuproine			80	200
2,2'-Biquinoline			5	250
4,4'-Dicarboxy-2,2'-biquinoline			N.E.	N.E.

N.E., no effect.

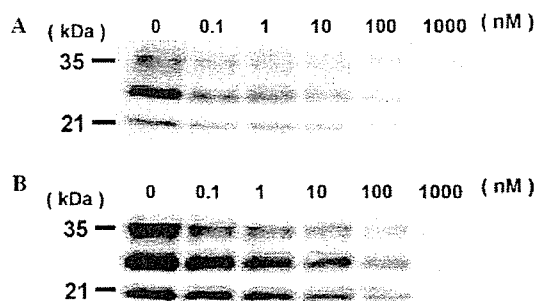
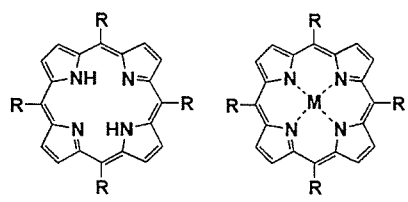
IC₅₀, concentration of a compound causing 50% inhibition of PrP-res formation relative to the control.

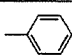
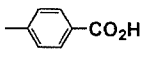
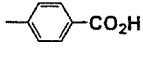
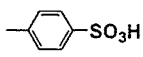
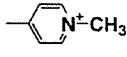
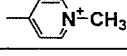
Figure 2. Anti-prion activity of 2,2'-biquinoline in prion-infected cells. Various concentrations of the compound were added to freshly passaged ScN2a cells (A) or F3 cells (B), and the PrP-res levels were analyzed by Western blotting. Lanes: 0, cells treated with DMSO alone; others, treated with the indicated concentration of 2,2'-biquinoline. Bars on the left indicate molecular mass markers at 35 and 21 kDa.

showed greater anti-prion activity than the metal-free compounds. Therefore, we examined whether SOD-like activity was associated with anti-prion activity, and discovered that this was the case.

PrP^C plays an important role in cell protection from oxidative stress, and modulates the activity of antioxidant enzymes by regulating the intracellular copper concentration, but it can also play a direct role owing to its intrinsic SOD activity.^{6,42,43} Cells with accumulated abnormal PrP^{Sc} displayed the phenotypes of decreased copper-binding capacity and higher sensitivity to oxidative stress.^{16,44} Interestingly, we found a significant correlation ($r = 0.93$) between SOD-like activity and anti-prion activity. Furthermore, we confirmed that the copper complex of D-penicillamine, which has been reported

Table 2. Inhibition of PrP-res formation in ScN2a cells and F3 cells by porphyrins



Compound	R	Metal(M)	Inhibition PrP-res IC ₅₀ (nM)	
			ScN2a cells	F3 cells
TPP			10	320
TCPP			250	160
Mn-TCPP (MnTBAP)		Mn ³⁺	40	60
TPPS			200	160
TMPyP			130	160
Mn-TMPyP		Mn ³⁺	5	40

IC₅₀, concentration of a compound giving 50% inhibition of PrP-res formation relative to the control.

Table 3. SOD-like activity of metal complexes

Chelating metal	Compound	SOD-like activity IC ₅₀ (μM)
Cu	8-Hydroxyquinoline	263
	Clioquinol	140
	Neocuproine	50
	Bathocuproine	32
	2,2'-Biquinoline	3
	4,4'-Dicarboxy-2,2'-biquinoline	263
	Cimetidine	0.4
	D-Penicillamine	28
Mn	TCPP	8
	TMPyP	0.3
Fe	TPEN	0.4

IC₅₀, concentration of a compound giving 50% inhibition of WST-1 reduction.

to show anti-prion activity, exhibits SOD-like activity.¹³

It is not easy to find molecules with both good metal-binding ability and high SOD-like activity, because, taking copper ions as an example, the former property

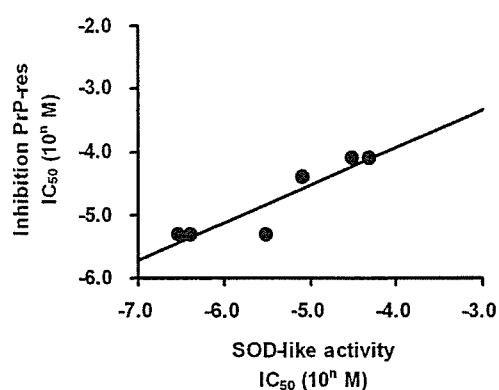


Figure 3. Correlation between SOD-like activity and inhibition of PrP-res formation in ScN2a cells. The plot shows data from seven compounds for which both SOD activity and inhibition of PrP-res formation were determined. ($r = 0.93$) SOD-like activity IC₅₀: concentration of a compound giving 50% inhibition of WST-1 reduction. Inhibition PrP-res IC₅₀: concentration of a compound giving 50% inhibition of PrP-res formation relative to the control.

means the Cu(II) complex is rather stable, while the latter property implies that the complex is prone to be reduced to the Cu(I)-chelator state.⁴⁵ This might explain why compounds such as clioquinol that are good copper chelators are nevertheless ineffective in terms of anti-prion activity.²⁵

On the other hand, cimetidine can form complexes with both Cu(I) and Cu(II), and has satisfactory SOD-like activity in both states, so it may be a good candidate for anti-prion activity. Furthermore, cimetidine can cross the blood–brain barrier to act in the central nerve system.⁴⁶ This type of compounds may provide a possible therapeutic approach for prion diseases.

In conclusion, we suggest that compounds which have copper-selective chelating ability, and whose copper complexes have high SOD-like activity are candidates for anti-prion drug.

References and notes

- Prusiner, S. B. *Science* **1982**, *216*, 136.
- Bounias, M.; Purdey, M. *Sci. Total Environ.* **2002**, *297*, 1.
- Brown, D. R.; Qin, K.; Herms, J. W.; Madlung, A.; Manson, J.; Strome, R.; Fraser, P. E.; Kruck, T.; von Bohlen, A.; Schulz-Schaeffer, W.; Giese, A.; Westaway, D.; Kretzschmar, H. *Nature* **1997**, *390*, 684.
- Viles, J. H.; Cohen, F. E.; Prusiner, S. B.; Goodin, D. B.; Wright, P. E.; Dyson, H. J. *Proc. Natl. Acad. Sci. U.S.A.* **1999**, *96*, 2042.
- Jackson, G. S.; Murray, I.; Hosszu, L. L.; Gibbs, N.; Waltho, J. P.; Clarke, A. R.; Collinge, J. *Proc. Natl. Acad. Sci. U.S.A.* **2001**, *98*, 8531.
- Brown, D. R.; Wong, B. S.; Hafiz, F.; Clive, C.; Haswell, S. J.; Jones, I. M. *Biochem. J.* **1999**, *344*, 1.
- Brown, D. R. *J. Neurosci. Res.* **1999**, *58*, 717.
- Pauly, P. C.; Harris, D. A. *J. Biol. Chem.* **1998**, *273*, 33107.

9. McKenzie, D.; Bartz, J.; Mirwald, J.; Olander, D.; Marsh, R.; Aiken, J. *J. Biol. Chem.* **1998**, *273*, 25545.
10. Brown, D. R.; Hafiz, F.; Glass-smith, L. L.; Wong, B. S.; Jones, I. M.; Clive, C.; Haswell, S. J. *EMBO J.* **2000**, *19*, 1180.
11. Kimberlin, R. H.; Millson, G. C.; Bountiff, L.; Collis, S. C. *J. Comp. Pathol.* **1974**, *84*, 263.
12. Pattison, I. H.; Jebbett, J. N. *Nature* **1971**, *230*, 115.
13. Sigurdsson, E. M.; Brown, D. R.; Alim, M. A.; Scholtzova, H.; Carp, R.; Meeker, H. C.; Prelli, F.; Frangione, B.; Wisniewski, T. *J. Biol. Chem.* **2003**, *278*, 46199.
14. Copper(II) perchlorate hexahydrate 98% and D-penicillamine were purchased from Sigma. Iron(II) sulfate heptahydrate, 2,2'-biquinoline, and cimetidine were purchased from Wako Pure Chemical (Osaka, Japan). 1,10-Phenanthroline monohydrate, 2,9-dimethyl-4,7-dimethyl-1,10-phenanthroline (bathocuproine), 2,9-1,10-phenanthroline (neocuproine), tetraphenylporphine (TPP), tetraphenylporphine tetrasulfonic acid (TPPS), $\alpha,\beta,\gamma,\delta$ -tetrakis(1-methylpyridinium-4-yl)porphine *p*-toluenesulfonate (TMPyP), tetrakis(4-carboxyphenyl)porphine (TCPP), 2,2'-bichinchonic acid dipotassium salt, 5-chloro-7-iodo-8-hydroxyquinoline (clioquinol), and 8-hydroxyquinoline were purchased from Tokyo Kasei (Tokyo, Japan). Manganese(III) tetrakis(1-methylpyridinium-4-yl)porphyrin pentachloride (Mn-TMPyP) and Mn(III)tetrakis(4-benzoic acid)porphyrin chloride (Mn-TCPP or Mn-TBAP) were purchased from Calbiochem (California, USA). They were dissolved in 100% dimethylsulfoxide (DMSO) or 95% ethanol just before use.
15. Two types of prion-infected mouse neuroblastoma (N2a) cell lines were used in this study: N2a cells infected with the RML strain (ScN2a) [16] and N2a#58 cells infected with the Fukuoka-1 strain (F3). N2a#58 cells are known to express five times more normal PrP than N2a cells. Both ScN2a cells and F3 cells were grown in six-well culture plates in Opti-MEM (Invitrogen) supplemented with 10% fetal bovine serum. The cells were allowed to reach confluence, and chemicals at various concentrations were added to the medium when 5% of the confluent cells were passaged. The final concentration of either DMSO or ethanol in the medium was less than 0.2%. The cultures were allowed to grow to confluence (3 or 4 days).
16. Milhavet, O.; McMahon, H. E.; Rachidi, W.; Nishida, N.; Katamine, S.; Mange, A.; Arlotto, M.; Casanova, D.; Riondel, J.; Favier, A.; Lehmann, S. *Proc. Natl. Acad. Sci. U.S.A.* **2000**, *97*, 13937.
17. The chelation study was carried out using Job's method.^{18,19} Solutions of 10 mM Cu(II) and each compound at a compound:Cu (II) ratio of 1:0 to 0:1 were prepared in ultrapure water (MilliQ; Millipore Co., Japan) or 95% ethanol, and λ_{max} of the copper complex was measured.
18. Vosburgh, W. C.; Cooper, G. R. *J. Am. Chem. Soc.* **1941**, *63*, 437.
19. Job, P. *Ann. Chim.* **1928**, *9*, 113.
20. Kolthoff, I. M. S.; Sandell, E. B. *Textbook of Quantitative Inorganic Analysis*; Pergamon Press: New York, 1959, The MacMillan Co.
21. Ueno, K.; Imamura, T.; Cheng, K. L. *Handbook of Organic Analytical Reagents*; Pergamon Press: Tokyo, 1992, CRC Press.
22. Birker, P. J.; Freeman, H. C. *J. Am. Chem. Soc.* **1977**, *99*, 6890.
23. The anti-prion activity of each compound was assayed by measuring the 50%-inhibitory concentration (IC₅₀) for PrP-res formation in ScN2a cells and F3 cells, as described in previous reports.^{24–26} Briefly, compounds were added at designated concentrations to the medium when cells were passaged at 10% confluency. The cells were allowed to grow to confluence and lysed with lysis buffer (0.5% sodium deoxycholate, 0.5% Nonidet P-40, and PBS). The lysates were digested with 10 $\mu\text{g}/\text{ml}$ proteinase K for 30 min at 37 °C and centrifuged at 15,000 rpm for 5 min at 24 °C with GLASSFOG(Q-bio gene, USA). The pellets were resuspended in sample loading buffer and boiled. Samples were separated by electrophoresis on 15% Tris-glycine-SDS-polyacrylamide gel and electroblotted. PrP-res was detected using an antibody, SAF83 (1:5000; SPI-Bio, France), followed by an alkaline phosphatase-conjugated secondary antibody. Immunoreactive signals were visualized using CDP-Star detection reagent (Amersham Biosciences Corp., U.S.A.) and were analyzed densitometrically. At least three independent experiments were performed to estimate IC₅₀ of each compound.
24. Doh-Ura, K.; Iwaki, T.; Caughey, B. *J. Virol.* **2000**, *74*, 4894.
25. Murakami-Kubo, I.; Doh-ura, K.; Ishikawa, K.; Kawatake, S.; Sasaki, K.; Kira, J.; Ohta, S.; Iwaki, T. *J. Virol.* **2004**, *78*, 1281.
26. Ishikawa, K.; Doh-ura, K.; Kudo, Y.; Nishida, N.; Murakami-Kubo, I.; Ando, Y.; Sawada, T.; Iwaki, T. *J. Gen. Virol.* **2004**, *85*, 1785.
27. Day, B. J.; Shawen, S.; Liochev, S. I.; Crapo, J. D. *J. Pharmacol. Exp. Ther.* **1995**, *275*, 1227.
28. Day, B. J.; Crapo, J. D. *Toxicol. Appl. Pharmacol.* **1996**, *140*, 94.
29. Younes, M.; Lengfelder, E.; Zienau, S.; Weser, U. *Biochem. Biophys. Res. Commun.* **1978**, *81*, 576.
30. Kimura, E.; Sakonaka, A.; Nakamoto, M. *Biochim. Biophys. Acta* **1981**, *678*, 172.
31. Kimura, E.; Yatsunami, A.; Watanabe, A.; Machida, R.; Koike, T.; Fujioka, H.; Kuramoto, Y.; Sumomogi, M.; Kunimitsu, K.; Yamashita, A. *Biochim. Biophys. Acta* **1983**, *745*, 37.
32. Wada, K.; Fujibayashi, Y.; Yokoyama, A. *Arch. Biochem. Biophys.* **1994**, *310*, 1.
33. Goldstein, S.; Czapski, G. *Free Radic. Res. Commun.* **1991**, *12–13*, 205.
34. Baudry, M.; Etienne, S.; Bruce, A.; Palucki, M.; Jacobsen, E.; Malfroy, B. *Biochem. Biophys. Res. Commun.* **1993**, *192*, 964.
35. Darr, D. J.; Yanni, S.; Pinnell, S. R. *Free Radic. Biol. Med.* **1988**, *4*, 357.
36. Wada, K.; Fujibayashi, Y.; Tajima, N.; Yokoyama, A. *Biol. Pharm. Bull.* **1994**, *17*, 701.
37. SOD-like assay kit-WST (Dojindo Chemical, Kumamoto, Japan) was used for the quantification of SOD-like activity. This method is a xanthine-based spectrophotometric assay using the tetrazolium salt WST-1. The SOD-like activity was evaluated using the standard curve of SOD-like activity versus absorbance at 450 nm. Differences of SOD-like activity were tested by use of the unpaired Student's *t* test, and *p* values smaller than 0.05 were considered to be statistically significant.
38. Kimura, E.; Koike, T.; Shimizu, Y.; Kodama, M. *Inorg. Chem.* **1986**, *25*, 2242.
39. Nagano, T.; Hirano, T.; Hirobe, M. *J. Biol. Chem.* **1989**, *264*, 9243.
40. Hijazi, N.; Shaked, Y.; Rosenmann, H.; Ben-Hur, T.; Gabizon, R. *Brain Res.* **2003**, *993*, 192.
41. Cherny, R. A.; Atwood, C. S.; Xilinas, M. E.; Gray, D. N.; Jones, W. D.; McLean, C. A.; Barnham, K. J.; Volitakis, I.; Fraser, F. W.; Kim, Y.; Huang, X.; Goldstein, L. E.; Moir, R. D.; Lim, J. T.; Beyreuther, K.;

- Zheng, H.; Tanzi, R. E.; Masters, C. L.; Bush, A. I. *Neuron* **2001**, *30*, 665.
42. Martins, V. R.; Mercadante, A. F.; Cabral, A. L.; Freitas, A. R.; Castro, R. M. *Braz. J. Med. Biol. Res.* **2001**, *34*, 585.
43. Rachidi, W.; Vilette, D.; Guiraud, P.; Arlotto, M.; Riondel, J.; Laude, H.; Lehmann, S.; Favier, A. *J. Biol. Chem.* **2003**, *278*, 9064.
44. Rachidi, W.; Mange, A.; Senator, A.; Guiraud, P.; Riondel, J.; Benboubetra, M.; Favier, A.; Lehmann, S. *J. Biol. Chem.* **2003**, *278*, 14595.
45. Li, Q. X.; Luo, Q. H.; Li, Y. Z.; Shen, M. C. *Dalton Trans.* **2004**, 2329.
46. Totte, J.; Scharpe, S.; Verkerk, R.; Neels, H.; Vanhaeverbeek, M.; Smits, S.; Rousseau, J. J. *Lancet* **1981**, *1*, 1047.

Styrylbenzazole derivatives for imaging of prion plaques and treatment of transmissible spongiform encephalopathies

Kensuke Ishikawa,* Yukitsuka Kudo,† Noriyuki Nishida,‡ Takahiro Suemoto,§ Tohru Sawada,§ Toru Iwaki¶ and Katsumi Doh-ura*

*Department of Prion Research, Tohoku University Graduate School of Medicine, Sendai, Japan

†Division of Telecommunication and Information Technology, Biomedical Engineering Research Organization, Tohoku University, Sendai, Japan

‡Division of Cellular and Molecular Biology, Nagasaki University Graduate School of Biomedical Sciences, Nagasaki, Japan

§BF Research Institute Inc., Osaka, Japan

¶Department of Neuropathology, Graduate School of Medical Sciences, Kyushu University, Fukuoka, Japan

Abstract

Recent prevalence of acquired forms of transmissible spongiform encephalopathies (TSEs) has urged the development of early diagnostic measures as well as therapeutic interventions. To extend our previous findings on the value of amyloid imaging probes for these purposes, styrylbenzazole derivatives with better permeability of blood–brain barrier (BBB) were developed and analyzed in this study. The new styrylbenzazole compounds clearly labeled prion protein (PrP) plaques in brain specimens from human TSE in a manner irrespective of pathogen strain, and a representative compound BF-168 detected abnormal PrP aggregates in the brain of TSE-infected mice when the probe was injected intravenously. On the other hand, most of the compounds inhibited abnormal PrP

formation in TSE-infected cells with IC₅₀ values in the nanomolar range, indicating that they represent one of the most potent classes of inhibitor ever reported. BF-168 prolonged the lives of mice infected intracerebrally with TSE when the compound was given intravenously at the preclinical stage. The new compounds, however, failed to detect synaptic PrP deposition and to show pathogen-independent therapeutic efficacy, similar to the amyloid imaging probes we previously reported. The compounds were BBB permeable and non-toxic at doses for imaging and treatment; therefore, they are expected to be of practical use in human TSE.

Keywords: amyloid imaging, anti-prion activity, pathogen strain, prion disease, styrylbenzazole derivatives.

J. Neurochem. (2006) **99**, 198–205.

The transmissible spongiform encephalopathies (TSEs) or prion diseases form a group of neurodegenerative disorders characterized by abnormal deposition of protease-resistant isoforms of prion protein (PrP) in the CNS (Prusiner 1991). TSEs are classified as sporadic, hereditary or environmentally acquired, and have become a serious public health issue because of the recent prevalence of acquired Creutzfeldt–Jakob disease (CJD), such as the variant form due to bovine spongiform encephalopathy (Will *et al.* 1996) and the iatrogenic form with cadaveric growth hormone or dura grafts (Brown *et al.* 2000). There is an urgent need to develop prophylactic and therapeutic interventions as well as diagnostic measures at the preclinical or early clinical stages of these incurable diseases.

We have previously reported that some amyloid imaging compounds, primarily derived from amyloid dyes such as

Received February 16, 2006; revised manuscript received May 25, 2006; accepted May 30, 2006.

Address correspondence and reprint requests to Dr Kensuke Ishikawa, Division of Prion Biology, Department of Prion Research, Tohoku University Graduate School of Medicine, 2–1 Seiryō-machi, Aoba-ku, Sendai 980-8575, Japan. E-mail: ishikawa@mail.tains.tohoku.ac.jp

Abbreviations used: AD, Alzheimer's disease; BBB, blood–brain barrier; BSB, (trans, trans)-1-bromo-2,5-bis-(3-hydroxycarbonyl-4-hydroxy)styrylbenzene; CJD, Creutzfeldt–Jakob disease; DMSO, dimethylsulfoxide; FDDNP, 2-(1-[6-[(2-fluoroethyl)(methyl)amino]-2-naphthyl]ethylidene)malononitrile; GSS, Gerstmann–Sträussler–Scheinker syndrome; ICR, Institute of Cancer Research; ID, injected dose; NT, not tested; PrP, prion protein; PrPres, protease-resistant PrP; PTA, phosphotungstic acid; PVDF, polyvinylidene difluoride; TSE, transmissible spongiform encephalopathy.

Congo red and thioflavin T, are useful for detection of prion plaques and treatment of TSE (Ishikawa *et al.* 2004). These compounds, however, are limited in their ability because of inefficient brain uptake. Here we describe new compounds, styrylbenzoazole derivatives, which have been developed for practical use and analyzed for their PrP imaging ability, anti-prion activity, therapeutic efficacy, brain uptake and toxicity.

Materials and methods

Chemicals and experimental models

All of the test compounds were synthesized at Tanabe R & D (Saitama, Japan) and used freshly after being dissolved in 100% dimethylsulfoxide (DMSO).

Cultured cells were grown in Opti-MEM (Invitrogen, Carlsbad, CA, USA) supplemented with 10% fetal calf serum. As cellular models of TSE, we used mouse neuroblastoma (N2a) cells persistently infected with the RML strain (ScN2a) (Race *et al.* 1988) and six other prion-infected cell lines: N2a58 cells individually infected with the RML strain, the 22L strain (Nishida *et al.* 2000) and Fukuoka-1 strain (Ishikawa *et al.* 2004); N2a cells infected with the 22L strain; mouse hypothalamic cells (GT1-7) infected with the 22L strain (Milhavet *et al.* 2000); and mouse fibroblast cells (L929) infected with the RML strain (Vorberg *et al.* 2004).

Tg7 mice overexpressing hamster PrP (Race *et al.* 1995) and Tga20 mice overexpressing mouse PrP (Fischer *et al.* 1996) were also used. These mouse models were intracerebrally infected with 20 μ L brain homogenate comprising 1% (w/v) of the 263K strain and the RML strain respectively. The Tg7 mice showed plaque-type PrP deposition between the cerebral cortex and hippocampus by 6 weeks after infection, followed by synaptic-type PrP deposition in the thalamus. The Tga20 mice showed similar pathological deposition, but plaques were not seen as frequently. Each mouse weighed \sim 30 g, and was maintained under deep ether anesthesia for minimum distress during all surgical procedures. Permission for the animal study was obtained from either the Animal Experiment Committee of Kyushu University or Tohoku University, Japan.

Brain uptake study

Test compounds were administered intravenously to Institute of Cancer Research (ICR) mice under ether anesthesia to determine initial brain uptakes. At 2 or 30 min after injection, the brains were removed, weighed and homogenized with saline. After centrifugation of the homogenate at 21 900 g for 10 min, the supernatant was applied to a conditioned C18 solid-phase extraction cartridge, and the compounds were eluted with methyl alcohol. Fluorescence was detected by high performance liquid chromatography with a fluorescence detector as reported previously (Okamura *et al.* 2005), and the percentage of injected dose per gram (%ID/g) was used as a measure of the level of the compounds in the brain.

In vitro PrP imaging in sections

Autopsy-diagnosed brain samples from cases of Gerstmann-Sträussler-Scheinker syndrome (GSS) ($n = 2$), sporadic CJD ($n = 5$), iatrogenic dura CJD with synaptic PrP deposition ($n = 1$) and non-TSE control cases with amyloid lesions [Alzheimer's disease (AD), $n = 2$] or without amyloid lesions (cerebral infarction, $n = 1$)

were obtained from the Department of Neuropathology, Kyushu University, Japan. After fixation in 10% buffered formalin for 2 weeks, each sample of TSE was immersed in 98% formic acid for the reduction of prion infectivity, embedded in paraffin and cut into sections 7 μ m thick. Sections of a variant CJD case were kindly provided by Dr James W. Ironside of the CJD Surveillance Unit, Edinburgh, UK. For neuropathological staining, deparaffinized sections were immersed in 1% Sudan black solution to quench tissue autofluorescence. They were then incubated for 30 min in 1- μ M solutions of the test compounds, rinsed with distilled water and examined under a fluorescence microscope (DMRXA; Leica Instruments, Wetzlar, Germany) with a UV or FITC filter set.

For comparison, each section was subsequently immunoassayed for PrP as described previously (Doh-ura *et al.* 2000). Briefly, the sections were treated with a hydrolytic autoclave and incubated with a rabbit primary antibody, c-PrP, which was raised against a mouse PrP fragment, amino acids 214–228 (1 : 200; Immuno-Biological Laboratories, Gunma, Japan), followed by incubation with a horseradish peroxidase-conjugated secondary antibody (1 : 200; Vector Laboratories, Burlingame, CA, USA). The reaction product was developed with 3,3'-diaminobenzidine tetrahydrochloride solution and counterstained with hematoxylin. Paraffin-embedded brains of experimental animals were similarly investigated.

In vivo PrP imaging in model animals

BF-168 (molecular weight 312.34) dissolved in 10% DMSO was administered intravenously (0.5–5 mg/kg body weight) into Tg7 mice at 6–7 weeks after injection when the mice showed no apparent clinical signs of TSE. As controls, vehicle alone was similarly injected into infected mice, and BF-168 was administered into uninfected mice. The animals were killed at various time points, and the brains were rapidly frozen and cut into coronal sections 10 μ m thick using a cryostat (CM3050; Leica Instruments). The sections were thaw-mounted on slides, dried and coverslipped. They were examined under a fluorescence microscope and further analyzed immunohistochemically as described above.

In vitro treatment in cell cultures

Abnormal PrP formation was assayed by the content of protease-resistant PrP (PrPres) in cellular models of TSE as described previously (Caughey and Raymond 1993). Each compound was added at the designated concentrations when cells were passaged at 10% confluence, while maintaining the final concentration of DMSO in the medium at $<$ 0.5%. The cells were allowed to grow to confluence and lysed with lysis buffer (0.5% sodium deoxycholate, 0.5% Nonidet P-40, phosphate-buffered saline). For analysis of PrPres, samples were digested with 10 μ g/mL proteinase K for 30 min, and the digestion was stopped with 0.5 mM phenylmethylsulfonyl fluoride. The samples were centrifuged at 100 000 g for 30 min, and pellets were resuspended in 1 \times sample loading buffer and boiled. For analysis of cellular PrP in N2a cells, cell lysates were mixed directly with a quarter volume of 5 \times sample loading buffer and boiled. These samples were separated by electrophoresis on a 15% Tris-glycine-sodium dodecyl sulfate polyacrylamide gel and electroblotted on to a polyvinylidene difluoride (PVDF) filter (Millipore, Bedford, MA, USA). PrP was detected using a monoclonal antibody, SAF83 (1 : 5000; SPI-BIO, Massy, France), followed by an alkaline phosphatase-conjugated

goat anti-mouse antibody (1 : 20 000; Promega, Madison, WI, USA). Immunoreactive blots were visualized with CDP-Star detection reagent (Amersham, Piscataway, NJ, USA). More than two independent assays were performed in each experiment and signals were analyzed using image analysis software. The approximate concentration of the compound giving 50% inhibition of PrPres formation, relative to the vehicle-treated control (IC_{50}), was estimated by signal intensity. To control for the detection limits of western blotting, we performed additional experiments utilizing sodium phosphotungstic acid (PTA) precipitation, which is the most sensitive technique presently available to detect PrPres (Safar *et al.* 1998). The PTA precipitation was undertaken on cell lysates of ScN2a treated with BF-168 at a designated concentration. The resulting pellets were collected by centrifugation and then analyzed by immunoblotting as described above.

In vivo treatment in model animals

BF-168 solution (4 mg/kg body weight) or vehicle alone was injected intravenously to experimental animals ($n = 5$) once a week. The treatment was started at 2 weeks after injection for Tg7 mice and at 4 weeks after injection for Tga20 mice, and repeated for 4 weeks. A continuous subcutaneous infusion of BF-168 was also given to Tga20 mice ($n = 5$) using an Alzet osmotic pump (Durect, Cupertino, CA, USA). In accordance with the manufacturer's instructions, each pump was filled with BF-168 solution at the designated doses and placed in a subcutaneous area of the back at 4 weeks after injection. The animals showed no apparent adverse effects of the treatment and were monitored 5 days a week until obvious clinical signs appeared. Statistical significance was analyzed by one-way ANOVA followed by Scheffé's method for multiple comparisons.

Results

Brain uptake and toxicity

We designed and synthesized novel styrylbenzoxazole derivatives (Table 1), styrylbenzothiazole and styrylbenzimidazole derivatives (Table 2) with more efficient permeability of the BBB and less toxicity. Values for brain uptake at 2 min after intravenous injection of the compounds were in the 2.4–17.0%ID/g range, indicating a satisfactory level for imaging probes. Their washouts from the brain varied, with the ratio of %ID/g at 2 min to that at 30 min after injection ranging from 1.0 to 56.9. Acute toxicity was tested by administering each compound intravenously at ~10 mg/kg body weight into normal ICR mice. No apparent toxic effect was observed with any of the compounds tested.

PrP imaging ability

Imaging of abnormal PrP deposition by the compounds was first performed in brain sections of human TSE. The compounds fluorescently labeled most of the PrP plaques in cerebellar cortices of both GSS cases (Fig. 1a, representative data). Among sections from the sporadic CJD cases, PrP deposition was labeled only in a case with plaques (Fig. 1c). In the cerebral cortex from the variant CJD case, large core plaques were detectable, whereas the majority of immunopositive aggregates were not labeled (Fig. 1e). In contrast, no fluorescence signal was identified in sections from the dura CJD case or the other sporadic CJD cases that

Table 1 Chemical structure, PrPres inhibition and brain uptake of styrylbenzoxazole derivatives including BF-168

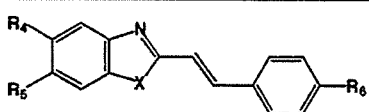
Compound	R ₁	R ₂	R ₃	IC ₅₀ (nM) ^a	Brain uptake (%ID/g) ^b		Ratio of 2 to 30 min brain uptake
					2 min	30 min	
BF-168	H	O(CH ₂) ₂ F	NH(CH ₃)	0.4	3.9 ^c	1.6	2.4
BF-125	H	H	N(C ₂ H ₅) ₂	10.2	3.0	3.0	1.0
BF-133	F	H	N(CH ₃) ₂	1.6	5.5	3.8	1.4
BF-135	NO ₂	H	N(CH ₃) ₂	< 1	NT ^d	NT	–
BF-140	F	H	NH ₂	< 1	5.5	1.1	5.0
BF-145	F	H	NH(CH ₃)	< 1	4.4	1.6	2.8
BF-148	H	F	N(CH ₃) ₂	< 1	NT	NT	–
BF-165	H	H	NH(CH ₃)	7.1	7.2	NT	–
BF-169	H	OH	NH(CH ₃)	2.4	NT	NT	–
BF-173	I	H	NH ₂	2.2	NT	NT	–
BF-180	I	H	NH(CH ₃)	8.5	2.4	1.8	1.3
BF-191	H	H	Cl	1.8	12.0	1.7	7.1
BF-208	H	H	F	< 1	11.0	0.53	20.8
N-282	H	H	N(CH ₃) ₂	2.1	4.0	1.7	2.4
N-407	H	H	H	< 1	17.0	0.99	17.2

^aIC₅₀, approximate concentration of a compound giving 50% inhibition of PrPres formation relative to the control in ScN2a cells.

^b%ID/g, percentage of injected dose per gram in the brains of normal mice.

^calready reported in the previous work (Okamura *et al.*, 2004).

^dNT, not tested.

Table 2 Chemical structure, PrPres inhibition and brain uptake of styrylbenzothiazole and styrylbenzimidazole derivatives


Compound	X	R ₄	R ₅	R ₆	IC ₅₀ (nM) ^a	Brain uptake (%ID/g) ^b		Ratio of 2 to 30min brain uptake
						2 min	30 min	
BF-124	S	H	H	N(C ₂ H ₅) ₂	18.1	2.4	2.5	1.0
BF-162	S	F	H	N(CH ₃) ₂	1.4	NT ^c	NT	-
N-276	S	H	H	N(CH ₃) ₂	< 1	NT	NT	-
N-438	S	H	H	H	< 1	11.0	2.0	5.5
BF-126	NH	H	H	N(C ₂ H ₅) ₂	21	7.2	0.16	45
BF-166	NH	F	H	N(C ₂ H ₅) ₂	1.1	NT	NT	-
N-457	NH	H	H	Cl	< 1	7.1	0.21	33.8
N-491	NH	H	H	H	1.9	7.4	0.13	56.9

^aIC₅₀, approximate concentration of a compound giving 50% inhibition of PrPres formation relative to the control in ScN2a cells.

^b%ID/g, percentage of injected dose per gram in the brains of normal mice.

^cNT, not tested.

included perivacuolar and/or synaptic PrP deposition (data not shown). Background staining was barely observed after rinsing off the excess compound. Immunohistochemical analysis of PrP revealed that the compounds achieved high-specificity labeling (Figs 1b, d and f). The compounds displayed no signal in control sections without amyloid lesions (data not shown).

Similar results were observed in experimental mice. PrP plaques were specifically labeled in brain sections of Tg7 mice infected with the 263K strain, and there was no PrP immunopositive reaction or fluorescence signal in brain sections of uninfected mice (data not shown). We performed *in vivo* experiments using presymptomatic Tg7 mice at a later stage of TSE. A typical image is shown in Fig. 1(g); peripheral administration of BF-168 fluorescently labeled plaques in the cerebral white matter, indicating that the compound efficiently entered the brain and bound to coarse PrP deposits. Subsequent immunostaining verified the specificity and sensitivity for PrP (Fig. 1h). Non-specific staining, such as cerebrovascular labeling, was occasionally observed at 4 h after injection of 5 mg/kg BF-168, but not after 8 h or more. The stability of the fluorescence signals was examined at various time points up to 24 h after injection and the dye-PrP complex remained visible at the latest time. In contrast, there was no significant labeling after an injection of BF-168 into uninfected animals, or after an injection of vehicle alone to terminally ill Tg7 mice. Similar results were obtained for Tga20 mice infected with the RML strain, although plaques were less frequently detected (data not shown).

Anti-prion activity *in vitro*

The anti-prion activities of the compounds were investigated using ScN2a cells, which are most commonly used for drug screening for TSE treatment. Styrylbenzoxazole derivatives,

including BF-168, were evaluated and confirmed to inhibit PrPres formation with IC₅₀ values in the nanomolar or subnanomolar range (Fig. 2a and Table 1). Styrylbenzothiazole and styrylbenzimidazole derivatives were similarly potent, in a dose-dependent manner, within a non-toxic dose range (~10 μM) (Table 2). Treatment with vehicle alone showed no inhibitory effect compared with untreated controls (Fig. 2a). We utilized PTA precipitation, which increases the sensitivity of western blotting, and confirmed the potency of BF-168 at a concentration of 10 times the IC₅₀. Furthermore, radiographic film was exposed to the blotted PVDF membranes for 10 times longer than usual before developing. No significant signals were visualized, whereas bands representing the vehicle-treated control were so strong as to be already saturated (Fig. 2b). To determine whether the efficacy was transient, ScN2a cells treated with 10 nM BF-168 were further cultured for 2 weeks in the absence of BF-168. PrPres signals never reappeared, even through four passages after discontinuation of the treatment (Fig. 2c). To exclude the possibility of interference with immunodetection, BF-168 solution at a final concentration of 10 nM was added to a lysate of untreated ScN2a cells before proteinase K digestion. PrP signals were not affected (data not shown). Nor was any alteration observed in cellular PrP level of N2a cells after treatment with 10 nM BF-168 (Fig. 2d).

To investigate whether the efficacy of the compounds depends on pathogen strain, we tested BF-168 in three N2a58 cell lines individually infected with different strains. As shown in Table 3, BF-168 was only effective in N2a58 cells infected with the RML strain, although the inhibitory activity was not as strong as in ScN2a cells (~1 μM). In contrast, BF-168 was ineffective in the same N2a58 cells infected with the 22L or Fukuoka-1 strains up to 10 μM, a dose at which the compound showed host cytotoxicity.

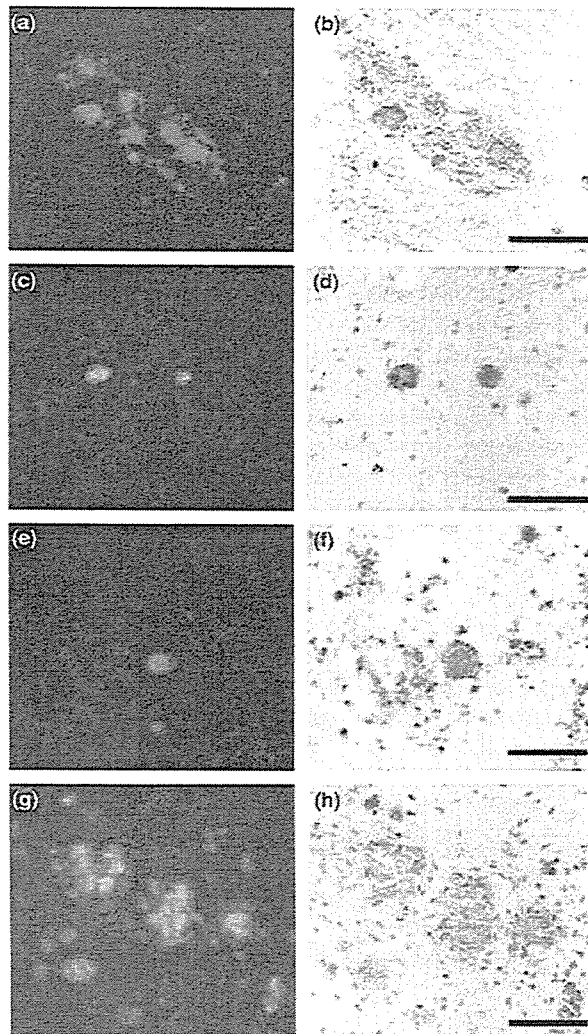


Fig. 1 PrP imaging *in vitro* and *in vivo*. BF-168 fluorescently labeled PrP deposition in a cerebellar section from the case of GSS (a), and in cerebral sections from cases of sporadic CJD with plaques (c) and variant CJD (e). Similar results were obtained from the brains of living TSE-infected mice that were intravenously injected with BF-168 solution (0.5 mg/kg). BF-168 detected PrP deposition in the cerebral white matter between the cortex and hippocampus (g). Sections (a, c, e and g) were subsequently immunoassayed for PrP (b, d, f and h). Bars represent 100 μm (a–f) and 25 μm (g and h).

Furthermore, we established L929 cells stably infected with the RML strain. BF-168 inhibited PrPres formation in the RML-infected L929 cells with an IC_{50} in the nanomolar range. We also tested potency against the 22L strain in two other cell lines, N2a and GT1-7 cells. BF-168 was ineffective in either cell line infected with the 22L strain. Other compounds tested here demonstrated similar results (data not shown). These results suggest that the styrylbenzoxazole derivatives exert their inhibitory activity on PrPres

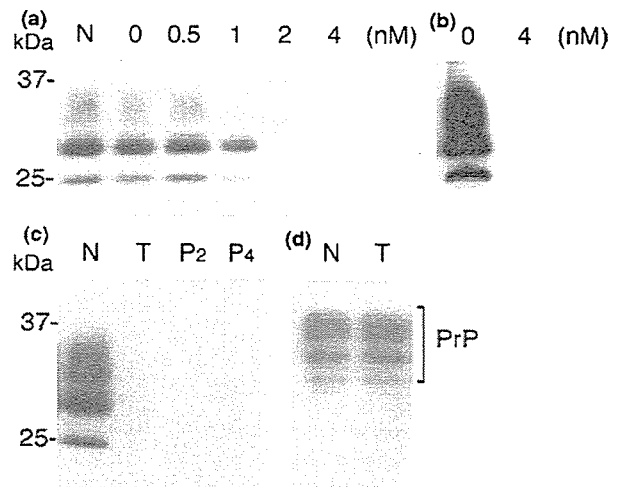


Fig. 2 Effects of BF-168 on PrP expression in ScN2a and N2a cells. BF-168 was added at the designated concentrations to freshly passaged cells. PrPres formation in ScN2a cells was inhibited in a dose-dependent manner (a). To exclude the sensitivity limit of immunoblotting, ScN2a cells treated with 4 nM BF-168 were also analyzed by sodium PTA, and no significant signals were visualized (b). ScN2a cells treated with 10 nM BF-168 were maintained for an additional four passages, and the PrPres signal was not restored in the absence of BF-168 (c). PrP expression was not affected in N2a cells that were grown in the presence of 10 nM BF-168 (d). Lane N, untreated cells; lane 0, cells treated with vehicle alone; lane T, cells treated with 10 nM BF-168; lanes P₂ and P₄, cells following two and four passages after treatment respectively. Bars on the left indicate molecular size markers at 37 and 25 kDa.

Table 3 Anti-prion activities (IC_{50}) of BF-168 in various types of TSE-infected cells

Host cells	Pathogen strains		
	RML	22L	Fukuoka-1
N2a	0.4 nM	None ^a	– ^b
N2a58	~ 1 μM	None	None
L929	~ 10 nM	–	–
GT1-7	–	None	–

^aNone, no significant PrPres inhibition up to 10 μM , a dose that affect the rate of cell growth.

^b, not available.

formation in a strain-dependent, but not a host cell-dependent, manner.

Therapeutic efficacy *in vivo*

The therapeutic activity of the compounds *in vivo* was assayed in two different mouse models using BF-168 as a representative. Treatment was initiated 2–4 weeks after TSE infection and repeated once a week for 4 weeks. The dosage at a single administration corresponded to a dose sufficient to detect PrP plaques. As shown in Table 4, there was no

Table 4 Effects of BF-168 treatment on intracerebrally TSE-infected mice

Mouse - pathogen strain	n	Dose (mg/kg/week)	Administration	Incubation period	
				Mean ±	SD (days)
Tg7 - 263K					
	7	Control	-	49.4 ± 1.9	
	5	Vehicle	i.v. ^a	50.2 ± 4.1	
	5	4	i.v.	52.2 ± 2.6	
Tga20 - RML					
	7	Control	-	66.6 ± 1.6	
	5	Vehicle	i.v.	64.8 ± 1.6	
	5	4	i.v.	72.2 ± 2.5*	
	5	10	s.c. ^b	66.0 ± 3.1	

* $p < 0.001$ versus the other groups.

^ai.v., intravenous injection of BF-168 once a week for 4 weeks from 2 weeks p.i. for Tg7, or 4 weeks p.i. for Tga20.

^bs.c., continuous subcutaneous infusion of BF-168 for 4 weeks from 4 weeks p.i.

significant difference in incubation periods between groups of Tg7 mice infected intracerebrally with the 263K strain, with or without treatment. In contrast, intravenous injection with 4 mg/kg BF-168 significantly prolonged the incubation period (~ 11.4%) of Tga20 mice intracerebrally infected with the RML strain.

In another trial, we used osmotic pumps filled with BF-168 solution, assuming that the route of administration is a key issue. The pump worked continuously for 4 weeks, and the total dosage for the duration was selected to correspond to two to three times that administered intravenously. Subcutaneous infusion of BF-168, however, did not prolong incubation periods of Tga20 mice intracerebrally infected with the RML strain (Table 4). There was no significant difference in incubation period in either group of infected mice between untreated controls and controls treated with vehicle alone.

Discussion

Our results show that styrylbenzoazole derivatives represent candidates for imaging probes as well as therapeutic drugs for TSE. It has been increasingly necessary to develop minimally non-invasive methods for recognizing early clinical infection and evaluating treatment of TSE. We have already focused on two β -amyloid imaging probes and reported them as potential agents for TSE (Ishikawa *et al.* 2004). The problem is, however, that they seemed to have practical limitations because of inadequate brain uptake and washout. Here, we confirmed that novel styrylbenzoazole derivatives clearly labeled PrP plaques *in vitro* and BF-168, the parent compound, entered the brain and labeled PrP plaques *in vivo*, even at a 20-fold lower dose than the probes we previously reported. In brain uptake studies, all of the compounds showed BBB permeability with >1%ID/g, which is proposed to be sufficient for neuroimaging probes. The

background staining of 0.5 mg/kg BF-168 was almost absent at 4 h after administration, suggesting excellent clearance from the brain.

Most of styrylbenzoazole derivatives labeled β -amyloid aggregates in AD specimens in this study (data not shown) as well as in the previous study on Alzheimer's (Okamura *et al.* 2004). This is also observed with 2-(1-[6-[(2-fluoroethyl)(methyl)amino]-2-naphthyl]ethylidene)malononitrile (FDDNP), one of the promising agents for imaging β -amyloid deposition. FDDNP has been reported to label PrP plaques in brain sections, and is a candidate for imaging PrP deposition (Bresjanac *et al.* 2003). These findings imply lack of disease specificity, but the compounds should still be useful for some types of TSE, because anatomical distributions of amyloid deposition are characteristically different between diseases. Pathological changes including amyloid deposition of AD brain are always observed in the hippocampus but not in the cerebellum, whereas those of TSE tend to be absent from the hippocampus but to be demonstrated in the cerebellum.

Styrylbenzoazole derivatives detected predominantly PrP plaques, especially in specimens of sporadic CJD with plaques and variant CJD. However, their ability to detect synaptic or perivacuolar PrP deposition remains inconclusive, until more sensitive investigations, such as autoradiography, are available. The compounds tested in this study can be used with radionuclides. ¹⁸F-radiolabeled BF-168, which has already been employed for labeling of β -amyloid deposits including both neuritic and diffuse plaques in AD brain (Okamura *et al.* 2004), may be a suitable tool for investigating whether PrP deposition, other than plaque type, can be detected.

This study demonstrated that styrylbenzoazole derivatives have more potent anti-prion activity than the amyloid imaging probes reported previously (Ishikawa *et al.* 2004). Although the neuropathological processes remain unclear, one of the most likely strategies for TSE treatment is a small-molecule drug that can enter the brain and inhibit abnormal PrP formation. It is important to emphasize that styrylbenzoazole derivatives have a wide concentration safety margin, and some were effective even at subnanomolar doses in ScN2a cells. Dozens of drug candidates for TSE have been reported to date but, as far as we know, the most potent inhibitor class for abnormal PrP formation in ScN2a cells is specific blocking antibodies with an IC₅₀ in the nanomolar range (Peretz *et al.* 2001).

BF-168 showed no apparent alteration in cellular PrP expression level in N2a cells, and also labeled abnormal PrP deposition both *in vitro* and *in vivo*. These data suggest that styrylbenzoazole derivatives might interact directly with abnormal PrP molecules to block the conversion of normal to abnormal PrP. The structure-activity relationship, examined by introducing side-chain or functional groups into the benzoazole and/or benzene rings, demonstrates that the inhibitory potency is not always the same, even among

closely related compounds (data not shown). Although we could not obtain any insight into inhibitory mechanisms, the efficacy of BF-168 was dependent on pathogen strain, and this is consistent with our previous work using three types of cell lines (Ishikawa *et al.* 2004). In an attempt to further explore strain dependency, we tested three different pathogen strains in one host cell line, and three different host cell lines with one pathogen strain. BF-168 inhibited abnormal PrP formation in all three types of RML-infected cells, including ScN2a cells. By contrast, BF-168 did not demonstrate any inhibitory activity in the 22L- or Fukuoka-1-infected cells. It is well known that prion strains differ in their biological profiles such as the degree of glycosylation and the conformation of PrP molecules. In the imaging experiments we confirmed that the compound bound to a certain type of abnormal PrP aggregates. Thus, it was assumed that the therapeutic efficacy might be based on blocking certain interactions between normal and abnormal PrP, and that BF-168 might recognize the PrP conformation. However, considering a discrepancy in the *in vivo* experiment between PrP imaging and treatment using infected Tg7 mice, these inferences remain unsupported and the precise mechanism of the strain-dependent efficacies needs to be elucidated.

Kocisko *et al.* (2004) reported that anti-prion activity *in vitro* does not always correlate with that *in vivo*. With *in vivo* testing, there are many variables, such as inoculation route, dosing protocol and pathogen strain. The efficacy differed according to the BF-168 administration route in Tga20 mice, even though the dose administered subcutaneously for the same duration was no less than that administered intravenously. This might be due to differences in stability and clearance of BF-168 in relation to the route of administration.

Most previous therapeutic investigations showed a significant benefit *in vivo* when the treatment was started before, or soon after, peripheral TSE infection. Although the efficacy of BF-168 was limited, it is noteworthy that we obtained significant results with peripheral administration at a later stage of the intracerebral infection. In addition, BF-168 showed excellent brain uptake and binding affinity towards PrP aggregates *in vivo*, even at a low dose, suggesting that the compound should be a good imaging probe for clinical use. In the treatment of infected Tga20 mice, BF-168 showed almost the same prolongation of the incubation period but with a 10-fold smaller dose than (trans, trans)-1-bromo-2,5-bis-(3-hydroxycarbonyl-4-hydroxy)styrylbenzene (BSB), which we reported previously as one of the amyloid imaging probes applicable for TSE (Ishikawa *et al.* 2004). BF-168 showed a low IC_{50} of 0.4 nM in treatment of ScN2a cells, whereas the IC_{50} of BSB was more than 1000-fold higher (1.4 μ M). We decided the dosing protocol for our experimental animals from *in vitro* data, including the ratio of these IC_{50} values, and from an *in vivo* imaging experiment in which 0.1 mg BF-168 per injection was enough to detect PrP deposition. It is also

necessary to consider washout of the compound from the brain. Further studies are required to examine issues such as dose-response relationships, administration time and dosing conditions. Furthermore, there was a problem in that administration frequency was limited because animal tail tissue was damaged by repetitive intravenous injections. In addition, it should be investigated whether compounds with slower washout from the brain are more suitable as therapeutic agents.

In conclusion, styrylbenzoazole derivatives efficiently entered the brain and labeled pathological PrP deposition, and demonstrated some anti-prion activities both *in vitro* and *in vivo*. Although their efficacy depended on the pathogen strain, these are a new class of compounds with potential as therapeutic drugs and imaging probes for TSE.

Acknowledgements

This study was supported by grants to KD from the Ministry of Health, Labour and Welfare (H16-kokoro-024) and the Ministry of Education, Culture, Sports, Science and Technology 13557118, 14021085, Japan. The authors thank Dr James W. Ironside of the CJD Surveillance Unit, Edinburgh, UK, for providing the variant CJD specimens.

References

- Bresjanac M., Smid L. M., Vovko T. D., Petric A., Barrio J. R. and Popovic M. (2003) Molecular-imaging probe 2-(1-[6-[(2-fluoroethyl)(methyl) amino]-2-naphthyl]ethylidene) malononitrile labels prion plaques *in vitro*. *J. Neurosci.* **23**, 8029–8033.
- Brown P., Preece M., Brandel J. P. *et al.* (2000) Iatrogenic Creutzfeldt–Jakob disease at the millennium. *Neurology* **55**, 1075–1081.
- Caughey B. and Raymond G. J. (1993) Sulfated polyanion inhibition of scrapie-associated PrP accumulation in cultured cells. *J. Virol.* **67**, 643–650.
- Doh-ura K., Mckada E., Ogomori K. and Iwaki T. (2000) Enhanced CD9 expression in the mouse and human brains infected with transmissible spongiform encephalopathies. *J. Neuropathol. Exp. Neurol.* **59**, 774–785.
- Fischer M., Rulicke T., Raeber A., Sailer A., Moser M., Oesch B., Brandner S., Aguzzi A. and Weissmann C. (1996) Prion protein (PrP) with amino-proximal deletions restoring susceptibility of PrP knockout mice to scrapie. *EMBO J.* **15**, 1255–1264.
- Ishikawa K., Doh-ura K., Kudo Y., Nishida N., Murakami-Kubo I., Ando Y., Sawada T. and Iwaki T. (2004) Amyloid imaging probes are useful for detection of prion plaques and treatment of transmissible spongiform encephalopathies. *J. Gen. Virol.* **85**, 1785–1790.
- Kocisko D. A., Morrey J. D., Race R. E., Chen J. and Caughey B. (2004) Evaluation of new cell culture inhibitors of protease-resistant prion protein against scrapie infection in mice. *J. Gen. Virol.* **85**, 2479–2483.
- Milhavet O., McMahon H. E., Rachidi W. *et al.* (2000) Prion infection impairs the cellular response to oxidative stress. *Proc. Natl Acad. Sci. USA* **97**, 13 937–13 942.
- Nishida N., Harris D. A., Vilette D., Laude H., Frobert Y., Grassi J., Casanova D., Milhavet O. and Lehmann S. (2000) Successful transmission of three mouse-adapted scrapie strains to murine neuroblastoma cell lines overexpressing wild-type mouse prion protein. *J. Virol.* **74**, 320–325.

- Okamura N., Suemoto T., Shimadzu H. *et al.* (2004) Styrylbenzoxazole derivatives for *in vivo* imaging of amyloid plaques in the brain. *J. Neurosci.* **24**, 2535–2541.
- Okamura N., Suemoto T., Furumoto S. *et al.* (2005) Quinoline and benzimidazole derivatives: candidate probes for *in vivo* imaging of tau pathology in Alzheimer's disease. *J. Neurosci.* **25**, 10 857–10 862.
- Peretz D., Williamson R. A., Kaneko K. *et al.* (2001) Antibodies inhibit prion propagation and clear cell cultures of prion infectivity. *Nature* **412**, 739–743.
- Prusiner S. B. (1991) Molecular biology of prion diseases. *Science* **252**, 1515–1522.
- Race R. E., Caughey B., Graham K., Ernst D. and Chescbro B. (1988) Analyses of frequency of infection, specific infectivity, and prion protein biosynthesis in scrapie-infected neuroblastoma cell clones. *J. Virol.* **62**, 2845–2849.
- Race R. E., Priola S. A., Bessen R. A., Ernst D., Dockter J., Rall G. F., Mucke L., Chescbro B. and Oldstone M. B. (1995) Neuron-specific expression of a hamster prion protein minigene in transgenic mice induces susceptibility to hamster scrapie agent. *Neuron* **15**, 1183–1191.
- Safar J., Wille H., Itri V., Groth D., Serban H., Torchia M., Cohen F. E. and Prusiner S. B. (1998) Eight prion strains have PrP(Sc) molecules with different conformations. *Nat. Med.* **4**, 1157–1165.
- Vorberg I., Raincs A., Story B. and Priola S. A. (2004) Susceptibility of common fibroblast cell lines to transmissible spongiform encephalopathy agents. *J. Infect. Dis.* **189**, 431–439.
- Will R. G., Ironside J. W., Zeidler M. *et al.* (1996) A new variant of Creutzfeldt–Jakob disease in the UK. *Lancet* **347**, 921–925.

Original Paper

Clusterin expression in follicular dendritic cells associated with prion protein accumulation

K Sasaki,^{1*} K Doh-ura,² JW Ironside,³ N Mabbott⁴ and T Iwaki¹

¹Department of Neuropathology, Neurological Institute, Graduate School of Medical Sciences, Kyushu University, Fukuoka 812-8582, Japan

²Division of Prion Biology, Department of Prion Research, CTAAR, Tohoku University School of Medicine, Sendai 980-8575, Japan

³National CJD Surveillance Unit, University of Edinburgh, Western General Hospital, Edinburgh EH4 2XU, UK

⁴Institute for Animal Health, Edinburgh EH9 3JF, UK

*Correspondence to:

Dr K Sasaki, Department of Neuropathology, Neurological Institute, Graduate School of Medical Sciences, Kyushu University, Fukuoka 812-8582, Japan.
E-mail: ksasaki@np.med.kyushu-u.ac.jp

Abstract

Peripheral accumulation of abnormal prion protein (PrP) in variant Creutzfeldt–Jakob disease and some animal models of transmissible spongiform encephalopathies (TSEs) may occur in the lymphoreticular system. Within the lymphoid tissues, abnormal PrP accumulation occurs on follicular dendritic cells (FDCs). Clusterin (apolipoprotein J) has been recognized as one of the molecules associated with PrP in TSEs, and clusterin expression is increased in the central nervous system where abnormal PrP deposition has occurred. We therefore examined peripheral clusterin expression in the context of PrP accumulation on FDCs in a range of human and experimental TSEs. PrP was detected immunohistochemically on tissue sections using a novel highly sensitive method involving detergent autoclaving pretreatment. A dendritic network pattern of clusterin immunoreactivity in lymphoid follicles was observed in association with the abnormal PrP on FDCs. The increased clusterin immunoreactivity appeared to correlate with the extent of PrP deposition, irrespective of the pathogen strains, host mouse strains or various immune modifications. The observed co-localization and correlative expression of these proteins suggested that clusterin might be directly associated with abnormal PrP. Indeed, clusterin immunoreactivity in association with PrP was retained after FDC depletion. Together these data suggest that clusterin may act as a chaperone-like molecule for PrP and play an important role in TSE pathogenesis. Copyright © 2006 Pathological Society of Great Britain and Ireland. Published by John Wiley & Sons, Ltd.

Keywords: prion; clusterin; follicular dendritic cell; immunohistochemistry; detergent autoclaving pretreatment; immune deficiency

Received: 26 January 2006
Revised: 18 March 2006
Accepted: 28 March 2006

Introduction

Transmissible spongiform encephalopathy (TSE) is the generic term for the fatal neurodegenerative diseases associated with abnormal prion protein (PrP) deposition in the central nervous system (CNS). Human TSE diseases include Creutzfeldt–Jakob disease (CJD), Gerstmann–Sträussler–Scheinker disease, fatal familial insomnia, and kuru. In cases of variant CJD, transmission is thought to have occurred from exposure to bovine spongiform encephalopathy (BSE)-contaminated meat via the oral route [1–3]. In cases of variant CJD and some animal TSE models, peripheral accumulation of abnormal PrP occurs in the lymphoreticular system, within the lymphoid follicles of spleens, lymph nodes, Peyer's patches, and tonsils [4–6]. In these regions, abnormal PrP accumulates on the surfaces of follicular dendritic cells (FDCs) from an early stage of the disease [7], followed by CNS involvement via the peripheral nervous system [8,9].

Clusterin (apolipoprotein J) is a heterodimeric glycoprotein and is expressed in a variety of mammalian tissues. It is considered to have a variety of functions,

including inhibition of complement-mediated cytotoxicity by binding to the membrane attack complex [10]; regulation of apoptosis [11]; and as a survival factor for germinal centre B cells [12]. We have reported that, during TSE disease, clusterin is associated with deposits of abnormal PrP in the CNS [13]. In the CNS of TSE-affected subjects, clusterin co-localizes with the extracellular plaque-type PrP deposits. Clusterin expression is also up-regulated within lesions of synaptic PrP deposition, even though no co-localization is observed. As clusterin interacts with a range of other molecules [14,15], these findings suggest that secreted clusterin might act as a chaperone-like molecule for PrP. Previous *in vitro* investigations have shown that clusterin is induced in astrocytes by PrP fragments reminiscent of the abnormal PrP isoform [16], and prevents their fibrillar aggregation [17].

FDCs also express clusterin [12]. Therefore we investigated whether clusterin expression in the lymphoreticular system is likewise affected by TSE infection, and associated with the extracellular accumulation of abnormal PrP on FDCs.

Materials and methods

Antibodies

The antibodies used included anti-human PrP C-terminal (rabbit polyclonal, IBL, Japan; raised against a peptide mapping to the C-terminus of human PrP, cross-reacts with mouse PrP), anti-human PrP N-terminal (rabbit, IBL; raised against a peptide mapping to the N-terminus of human PrP, cross-reacts with mouse PrP), anti-human PrP (mouse monoclonal, 3F4, Signet, MA, USA; recognizing amino acid residues 109–112, cross-reacts with hamster PrP), anti-mouse clusterin (goat polyclonal, M-18, Santa Cruz, CA, USA; raised against a peptide mapping to the C-terminus of mouse clusterin), anti-human clusterin (goat, C-18, Santa Cruz; raised against a peptide mapping to the C-terminus of human clusterin), or anti-human clusterin (goat, Chemicon, CA, USA; raised against a purified clusterin from human plasma), anti-mouse CD21/CD35 (CR2/CR1, rat monoclonal, 7G6, PharMingen, CA, USA), anti-human CD35 (CR1, mouse, Ber-MAC-DRC, Dako, Denmark). We assessed two anti-human clusterin antibodies by immunohistochemistry and verified that both gave similar results [13].

Mouse models

Non-transgenic NZW mice and transgenic Tga20 mice [18,19] that express high amounts of mouse PrP were inoculated intraperitoneally (i.p.) with the Fukuoka-1 mouse-passaged scrapie agent strain (NZW/Fu-1, Tga20/Fu-1, respectively). Transgenic Tg7 mice [8,20] that express high amounts of hamster PrP on a mouse-PrP knockout background were inoculated i.p. with the 263K hamster-passaged scrapie agent strain (Tg7/263K). Permission for these animal experiments was obtained from the Animal Experiment Committee of Kyushu University.

Where indicated, C57BL/Dk mice were inoculated either orally or i.p. with the ME7 mouse-passaged

scrapie agent strain (C57BL/ME7 mice). To deplete FDCs temporarily, C57BL/Dk mice were given a single i.p. injection of a fusion protein containing the soluble lymphotoxin β receptor domain linked to the Fc portion of human IgG1 (LT β R-Ig) or 100 μ g polyclonal human IgG (hu-Ig) (Sandoglobulin[®]) as a control [21,22]. Where indicated, treatment was given 3 days before (–3 dpi) oral inoculation, or 14 or 42 days after (14 dpi & 42 dpi, respectively) i.p. inoculation with the ME7 scrapie agent strain as described [21,22]. Spleens were analysed 3 days after treatment; Peyer's patches were analysed 70 days after inoculation with the scrapie agent. Mice deficient in interleukin- (IL-) 6 (IL-6-knockout (KO) mice, on a 129/Sv \times C57BL/6 background) possess FDC networks but have impaired germinal centres [23]. IL-6-KO mice, and 129/Sv \times C57BL/6 immunocompetent wild-type mice, were also inoculated i.p. with the ME7 mouse-passaged scrapie agent strain. Permission for these animal experiments was obtained from the Ethical Review Committee at the Institute for Animal Health, Edinburgh, UK.

Table 1 summarizes the profiles of the mouse lines used in this study.

Human CJD cases

Paraffin-embedded sections of spleens, lymph nodes, appendices, and tonsils were examined from five cases of variant CJD (three males, two females, age range 17–39 years, duration of clinical illness 7–33 months) from the UK National CJD Surveillance Unit, University of Edinburgh, UK. Spleen sections were also examined from four cases of sporadic CJD (two males, two females, age range 55–69 years, duration of clinical illness 4–30 months) from the Department of Neuropathology, Kyushu University. The diagnosis of variant or sporadic CJD was confirmed by postmortem examination. Each case had consent for use of autopsy tissues for research purposes and local Ethics Committee approval for the use of human autopsy tissues from patients with CJD for research was also obtained.

Table 1. Profiles of mouse lines

Line	Background	Modification of PrP expression	PrP ^c on FDCs	Reference	Inoculum	PrP ^{sc} on FDCs
NZW wild		None	+		Fukuoka-1	+
C57BL/Dk Wild		None	+		ME7	+
Tg7	C57BL/10	MoPrP knockout Overexpress HaPrP under control of the endogenous MoPrP promoter	+	8,20	263K	–
Tga20	129/Sv \times C57BL/6	MoPrP knockout Overexpress MoPrP under control of the endogenous MoPrP promoter	–*	18,19	Fukuoka-1	–
IL-6 KO	129/Sv \times C57BL/6	None	+	23	ME7	+

MoPrP = mouse PrP; HaPrP = hamster PrP; PrP^c = cellular PrP expression on the FDCs; PrP^{sc} = abnormal PrP accumulation on FDCs of scrapie affected mice; (–) negative; (+) positive.

* Negative on FDCs but some cells within the paracortical T-cell area express PrP^c [19].

The inocula indicated were applied to the respective mouse lines in this study.

Immunohistochemistry

To enhance the detection of PrP by immunohistochemistry (IHC), formalin-fixed, paraffin-embedded sections were pretreated by hydrolytic autoclaving (1–2 mM HCl, 121 °C, 10 min) or a protocol using formic acid, guanidine thiocyanate, and hydrated autoclaving as previously reported [24,25]. We also performed an autoclaving pretreatment with Target Retrieval Solution (Dako) or buffer solution with detergent. A variety of detergents were examined including, Triton X-100 and Tween-20 as non-ionic detergents and sodium dodecyl sulphate as an ionic detergent. We found that non-ionic detergents enhanced PrP detection to a similar degree, whereas the ionic detergent enhanced PrP detection sensitivity, but caused considerable tissue damage. Autoclaving the sections in 0.1% Triton X-100 in 50 mM Tris-HCl, pH 7.6, 121 °C, 20 min, was found to be the most suitable method for the detection of abnormal PrP accumulation on FDCs, and was used in this study (hereinafter referred to as the detergent autoclaving method). Increased concentrations of Triton X-100 up to 0.5% did not significantly increase the signal intensity of the PrP detected or affect the degree of tissue damage. This indicated that the detergent autoclaving method had a wider range of optimum detergent concentrations than the HCl in the hydrolytic autoclaving method. Immunoreactions were visualized using diaminobenzidine as a chromogen.

To examine the co-localization of two different proteins on the same section, the first immunoreaction was visualized using 3-amino-9-ethylcarbazole (AEC; Vector, CA, USA), mapped, and photographed. The section was then decolourized by immersing it in ethanol, and the second immunohistochemical procedure was

performed with the other primary antibody. Double immunofluorescence was also performed to reveal sites of co-localization.

Results

Experiments demonstrated that the detergent autoclaving method was the most useful for detecting PrP by IHC. This was particularly evident on sections of spleen tissue, where this method drastically improved the signal intensity for PrP accumulated on FDCs in comparison with sections treated by the HCl autoclave method (Figure 1A and B, respectively). Table 2 shows comparisons between this detergent autoclaving method and conventional techniques for IHC detection of PrP. On human brain samples, most of the different types of PrP deposition could be detected by the detergent autoclaving method as well as by conventional techniques (Figure 1C and 1D, respectively). However, the detergent autoclaving method

Table 2. Comparison of the methods of immunohistochemistry for PrP

	Detergent autoclaving	HCl autoclaving [24]	Three steps [25]
PrP signal intensity			
Synaptic	+ ~ ++	++	+ ~ ++
Plaque	++	++	++
FDCs (mouse)	++	+	++
Background	Low	High	Moderate
Tissue damage	Low	High	Moderate
Simplicity	Simple	Moderate	Complicated

(+) positive; (++) strongly positive.

In the three steps method samples are pretreated with formic acid, guanidine thiocyanate, and hydrated autoclaving.

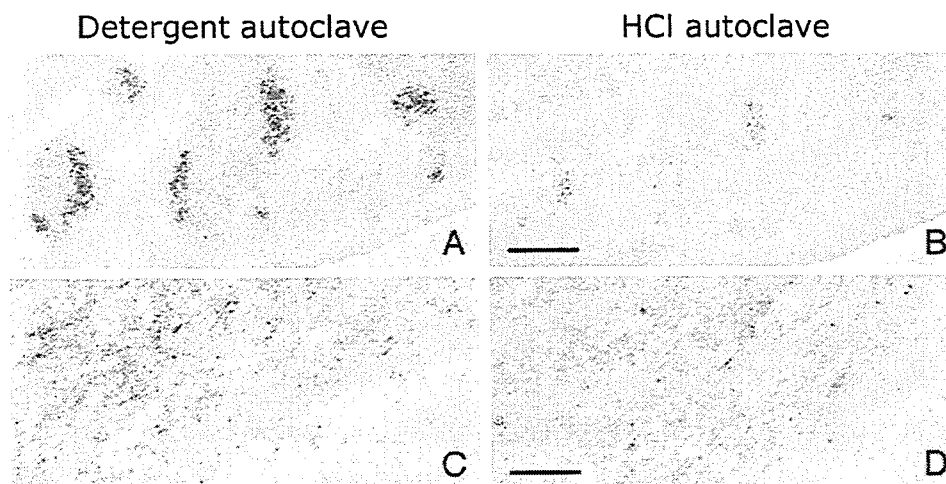


Figure 1. Effect of detergent autoclaving pretreatment on the detection of PrP by immunohistochemistry. (A, B) Serial sections of spleen from TSE-infected mice (NZW mouse inoculated with Fukuoka-1 strain) were immunostained for PrP. The detergent autoclaving method (A) dramatically increased the signal intensity of the PrP immunoreaction and lowered non-specific background staining in comparison with the HCl autoclaving method (B). (C, D) Serial sections of cerebral cortex from a case with sporadic CJD immunostained for PrP. Immunoreactivity for PrP is rather weak on sections pretreated by the detergent autoclaving method (C) in comparison with those pretreated by the HCl autoclaving method (D). However, abnormal fine granular deposits of PrP are detected by both methods. Bars: 200 µm (A, B), 100 µm (C, D)

decreased background staining, which facilitated the double immunofluorescence technique in this study.

We examined the lymphoreticular system of mouse models of TSE. In the spleens of scrapie agent-inoculated NZW/Fu-1 ($n = 5$) and C57BL/ME7 mice ($n = 3$), abnormal PrP accumulated on the dendritic network of FDCs as the disease progressed (Figure 2E), but not in the spleens of uninoculated NZW mice ($n = 5$) (Figure 2B) or scrapie agent-inoculated Tg7/263K ($n = 5$) or Tga20/Fu-1 mice ($n = 3$) (data not shown). The apparent lack of cellular

PrP expression by FDCs in the spleens of Tga20 mice probably prevents abnormal PrP amplification on these cells [19]. Likewise, after high-dose scrapie inoculation into these transgenic mice, neuroinvasion probably occurs via a putative 'direct neuroinvasion' pathway without the need for prior amplification of abnormal PrP on FDCs [8]. In uninoculated NZW mice, clusterin was constitutively and diffusely expressed in the reticular cells in lymphoid follicles (Figure 2A), as previously reported [26]. However, in the spleens of NZW/Fu-1 mice immunoreactivity for clusterin was

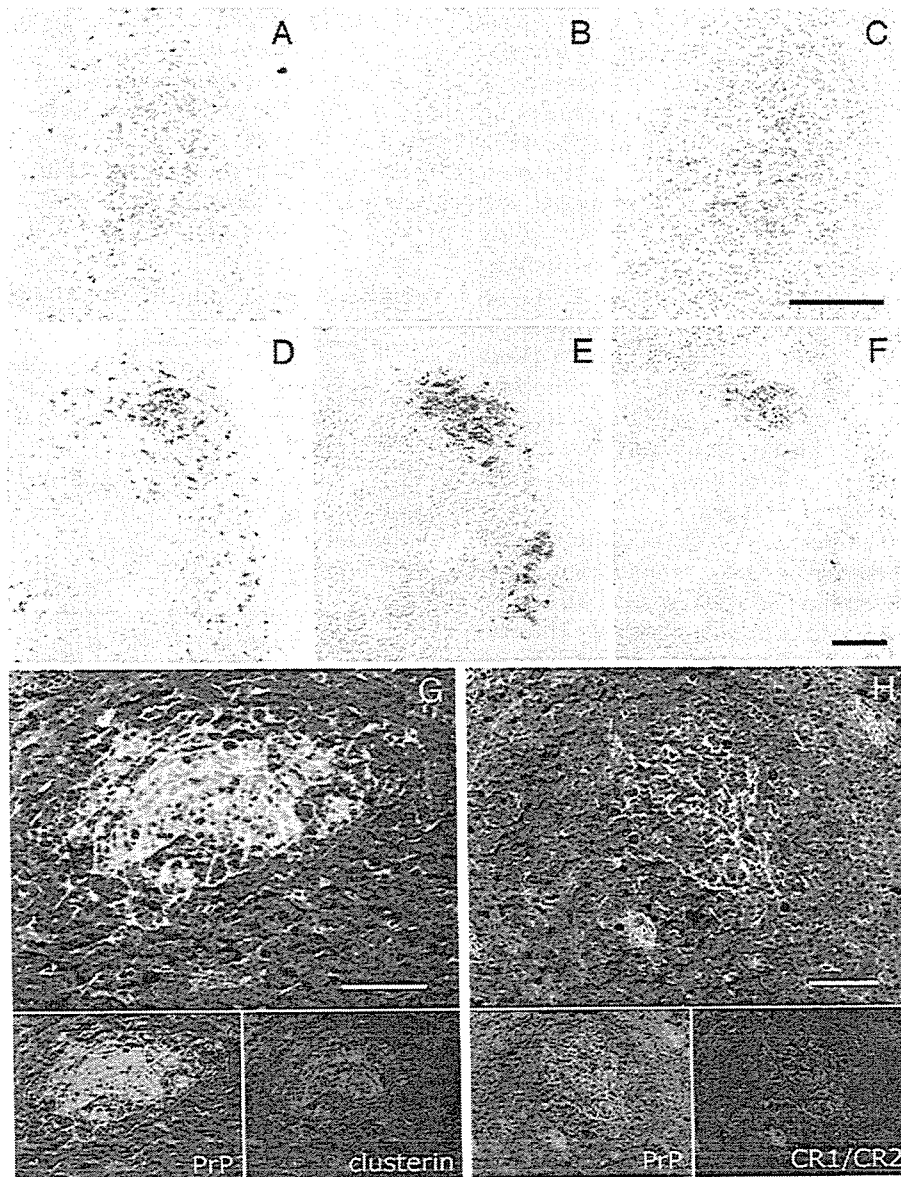


Figure 2. Immunohistochemistry for clusterin expression on FDCs in the spleens of uninoculated and scrapie-inoculated mice. (A–C) Serial sections of uninoculated NZW mouse spleen were immunostained for clusterin (A), PrP (B), and CR1/CR2 (C). Clusterin is constitutively expressed in the reticular cells in the lymphoid follicles of uninoculated mice (A) and not obviously condensed on the dendritic network of FDCs (C). However, increased clusterin expression was observed on FDCs from scrapie-inoculated mice. (D–F) The same section of spleen from the NZW/Fu-1 TSE mouse model was serially immunostained for clusterin (D), PrP (E), and CR1/CR2 (F). Immunoreactivity for clusterin is markedly condensed and increased on the FDCs associated with abnormal PrP accumulation. Similar results were observed in the C57BL/ME7 mouse model. The co-localization of these proteins was also confirmed by double immunofluorescence (G, H). (G) Clusterin (red) and PrP (green). (H) CR1/CR2 (red) and PrP (green). Bars: 100 μm (A–F), 50 μm (G, H)

condensed (Figure 2D) and co-localized with the PrP (Figure 2E) accumulated on the complement receptor 1/2 (CR1/CR2)-immunopositive dendrites [27] of FDCs (Figure 2F). No such accentuation of clusterin expression was observed in the spleens of scrapie-inoculated Tg7/263K mice or Tga20/Fu-1 mice (data not shown). The co-localization of clusterin and PrP on the FDCs was also confirmed by double immunofluorescence (Figure 2G and H).

Although the increased clusterin immunoreactivity mostly correlated with the abnormal PrP accumulations on splenic FDCs from scrapie-agent inoculated C57BL/ME7 mice, temporary FDC depletion 14 or 42 days after scrapie-agent inoculation [21,22] did not affect the association of clusterin with abnormal PrP (Table 3). Similarly, in the spleens of scrapie agent-inoculated IL-6-KO mice, immunoreactivity for clusterin was mostly correlated with abnormal PrP accumulation (Table 3) despite the impaired germinal centre development in these mice [23].

In Peyer's patches, increased clusterin expression was seen not only on the PrP-immunopositive FDCs of infected mice but also in the lymphoid follicles without PrP deposition (Table 3). Clusterin-labelled lymphoid follicles were also confirmed in the Peyer's patches of non-infected control mice (data not shown), but this occurred to a lesser extent than in TSE-infected mice.

Increased clusterin expression associated with the abnormal PrP deposition on FDCs was also observed in cases of human variant CJD. The extent and

intensity of clusterin immunoreactivity did not appear to be related to the age of the patient, or the duration of the clinical illness of the five cases examined (patient ages 17, 29, 33, 36, and 39 years; duration of clinical illness 33, 7, 18, 15, and 14 months, respectively). In each case, immunoreactivity for clusterin was increased wherever abnormal PrP accumulation on the FDCs was found, such as in the spleens, lymph nodes, appendices, and tonsils (Figure 3). In appendices, clusterin immunoreactivity was also increased in the lymphoid follicles without PrP deposition (Figure 3C and D), which was consistent with data from analysis of Peyer's patches of mouse TSE models. No increased clusterin immunoreactivity was observed on FDCs from sporadic CJD cases (data not shown) in which no PrP deposition was detected, except on appendices where clusterin immunoreactivity was increased on the FDCs even in non-CJD control cases (Figure 3E and F).

Discussion

Here we show that clusterin expression on FDCs is increased during TSE diseases and occurs in association with abnormal PrP accumulation. The dendritic network pattern of the clusterin immunoreactivity in the lymphoid follicles was associated with PrP accumulation on FDCs in NZW/Fu-1 mice and C57BL/ME7 mice. The increased clusterin immunoreactivity was mostly dependent on the presence of

Table 3. Effect of FDC depletion and impaired germinal centre development on clusterin expression in TSE-inoculated mice

	Immune deficiency	PrP IR	Clusterin IR*	CR1/CR2 IR	Effect on disease transmission†
					Intraperitoneal
Spleens					
Uninfected					
	LT β R-Ig	FDCs depleted	–	–	n/a
	Hu-Ig	Control	–	+	n/a
14 dpi					
	LT β R-Ig	FDCs depleted	–	–	Delayed [21]
	Hu-Ig	Control	+–	+	
42 dpi					
	LT β R-Ig	FDCs depleted	+	–	Delayed [21]
	Hu-Ig	Control	+	++	
	IL-6-KO	Impaired germinal centres	++	++	No effect [23]
	Wild-type	Control	++	++	
					Oral
Peyer's patches					
–3 dpi					
	LT β R-Ig	FDCs depleted	–	+‡	n.d.
	Hu-Ig	Control	+	+‡	n.d.

FDCs were depleted by treatment with LT β R-Ig, or Hu-Ig as a control [28]. Ig treatment was performed on the indicated days relative to scrapie challenge. Three mice were examined and estimated the immunoreactivity on each immune-deficient group (LT β R-Ig treated or IL-6 KO) or control group.

IR = immunoreactivity; dpi = days post scrapie inoculation; n.d. = not determined; n/a = not applicable; (–) = negative; (+–) = faint; (+) = positive; (++) = strongly positive.

* Immunoreactivity in the dendritic-network pattern.

† Data from previous reports [21–23].

‡ Clusterin immunoreactivity does not always correlate with PrP deposition; increased clusterin expression is also seen in some lymphoid follicles without PrP accumulation.

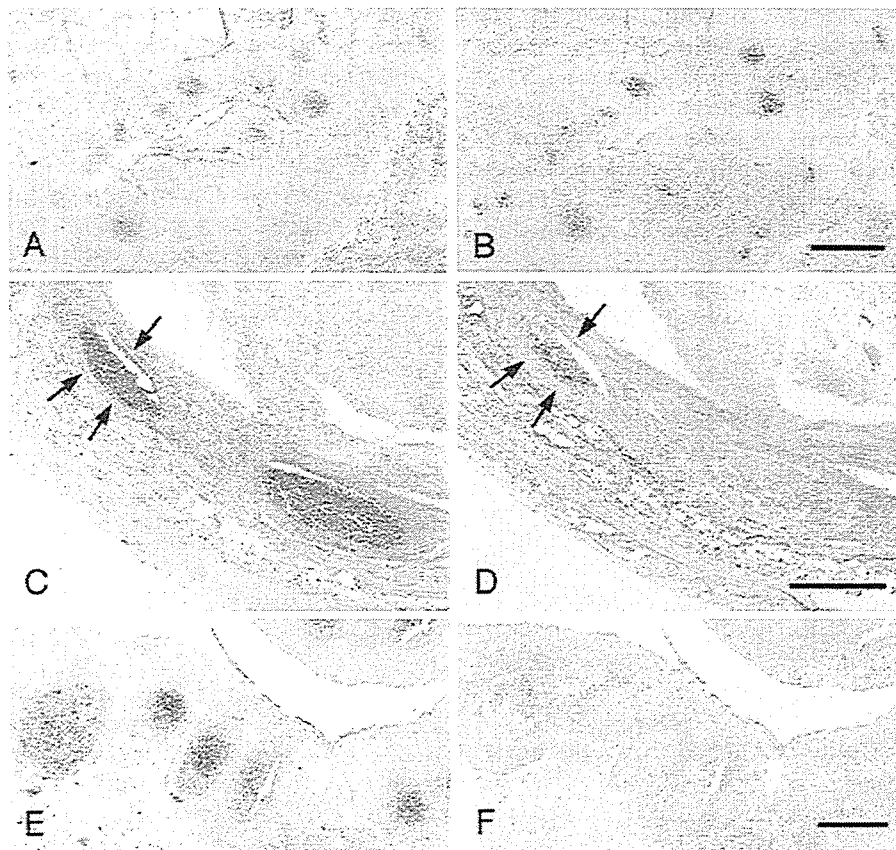


Figure 3. Immunohistochemistry of lymphoreticular tissues from human variant CJD and control (non-CJD) cases. (A, C, E) Clusterin. (B, D, F) PrP. (A, B) Serial sections of the tonsil from a variant CJD case. Clusterin immunoreactivity is increased on FDCs where abnormal PrP deposits are detected. (C–F) Serial sections of appendices from a variant CJD case (C, D) and a control case (E, F). Note that not only the lymphoid follicles with PrP accumulation (arrows) but also those without PrP accumulation show increased clusterin expression. Bars: 500 μ m

abnormal PrP deposition, irrespective of the TSE agent strains, host mouse strains, or various immune deficiencies. Moreover, clusterin accumulation was also seen in human variant CJD cases, which was consistently accompanied by PrP deposition on FDCs in the lymphoreticular system (except for the intestinal lymphoid follicles). We have previously reported that clusterin expression in the cerebrum was increased in association with increased PrP deposition [13]. The results in the present report provide evidence that clusterin accumulation also occurs in peripheral lymphoid tissues. Although a direct interaction between clusterin and PrP remains to be confirmed, these data suggest that clusterin may play an important role in the pathogenesis of TSE diseases in lymphoid tissues.

To determine whether clusterin was associated with abnormal PrP, we analysed the effect of FDC depletion on clusterin accumulation. Signalling through the $LT\beta R$ provides important stimuli for FDC maturation and maintenance. Blockade of this stimulation through treatment with $LT\beta R$ -Ig causes the temporary de-differentiation of FDCs [28]. In this study, CR1/CR2 expression on FDCs was certainly affected by $LT\beta R$ -Ig treatment in comparison with the control mice treated with Hu-Ig (Table 3), confirming that the

FDCs were temporarily de-differentiated. In uninoculated mice, clusterin expression by FDCs is down-regulated by $LT\beta R$ signalling blockade and undetectable by immunohistochemistry within two days of FDC depletion [12]. However, in this study we show that the detection of clusterin in the spleens of scrapie-inoculated mice was unaffected by FDC depletion and remained in close association with abnormal PrP (Table 3). These data imply that clusterin associates directly with abnormal PrP molecules exposed extracellularly on the surface of FDC dendrites.

Why clusterin expression is up-regulated during TSE disease is not known. Data from both human and experimental studies demonstrate that TSE infections induce the expression of both early and terminal complement components within the brain. However, the membrane attack complex (C5b–C9) is not involved in TSE pathogenesis [29]. Thus it is plausible that, during TSE diseases within the CNS, clusterin might be expressed as part of an innate response to inactivate the membrane attack complex formed by the terminal complement components [10], and to help protect neurons from potential complement-mediated lysis. It is also plausible that clusterin might be induced to exert anti-amyloidogenic properties [30]. Because